Lightning Phenomenology Notes

Note 20

8 June 1999

Leader-Pulse Step-Formation Process

Carl E. Baum
Air Force Research Laboratory
Directed Energy Directorate

Abstract

A fundamental part of a lightning event is the leader coming down from the cloud and the leader up from the earth, including the case of a triggering rocket. These leaders often have a stepping behavior, during which the propagation speeds are larger than the average speed of leader propagation. This paper expands on the previously developed corona model for a nonlinear transmission line to include both forward and backward propagating current pulses during the leader pulse. Based on measured electromagnetic data the ratio of leader-tip speed during the leader pulse to the average speed is estimated. This is combined with reported optically measured average speeds to estimate the leader-tip speed which is observed to be consistent with the model.

1. Introduction

In natural lightning and triggered lightning there are fast impulsive events often called steps that are a fundamental part of the discharge process. These include the stepped leader, both downward propagating (usually negative) from the cloud and upward propagating (usually positive) from the ground including field-enhancement devices such as a small rocket and wires to initiate the streamer.

There are various publications which present optical data concerning such steps. For downward (negative) leaders, Schonland [6] reports 0.8×10^5 to 2.4×10^6 m/s for average speed and estimates that the speed during the steps exceeds 5×10^7 m/s. Note that in these measurements the best time resolution of the camera is quoted as 0.7 μs. Berger [7] reports average speeds from 0.85×10^5 to 1×10^6 m/s. More discussion is given in [10].

There are also reports of leader speeds for upward (positive) leaders. For rocket-triggered lightning Idone [8] reports optically measured average speeds of 1.2×10^5 to 9.4×10^5 m/s. Also reported are lower bounds of 5×10^7 and 6×10^7 m/s for two steps (backward propagating during the leader development. The time resolution of the camera is quoted as about 3 μs. Berger [7] also reports positive leaders propagating upward from towers with average speeds from 0.4×10^5 to 1×10^6 ms.

Section 5 shows some stepping behavior with 10 ns resolution as measured from the radiated electromagnetic fields. This can be used to determine the fractional time spent during steps and thereby estimate the ratio of the speed during the steps to the average speed.

2. Nonlinear Transmission-Line Modelling of Lightning processes

In [1, 5] a nonlinear transmission-line model based on an equivalent corona radius Ψ_c, in turn based on a breakdown electric field E_b, is developed. The telegrapher equations become (no resistive losses)

$$\frac{\partial}{\partial z}\left(\frac{Q'}{C'}\right) = -\, L'\frac{\partial t}{\partial t}$$
$$\frac{\partial I}{\partial z} = -\,\frac{\partial Q'}{\partial t} \qquad (2.1)$$
$$I = \text{current}$$
$$Q' \equiv \text{charge per unit length}$$

Note the use of Q' instead of voltage V. Here we have

$$L' = \frac{\mu_0}{2\pi}\,\ell n\left(\frac{\Psi_\infty}{\Psi_0}\right) \equiv \text{inductance per unit length}$$

$$C' = 2\pi\varepsilon_0\,\ell n^{-1}\left(\frac{\Psi_\infty}{\Psi_c}\right) \equiv \text{capacitance per unit length}$$

$\Psi_0 \equiv$ radius of central arc carrying most of the current (2.2)

$\Psi_c \equiv$ corona radius locating the charge per unit length

$\Psi_\infty \equiv$ effective radius of return path for current as used in thin-wire antenna theory

with the approximations

$$0 < \Psi_0 \le \Psi_c << \Psi_\infty$$
$$\Psi_c = \frac{|Q'|}{2\pi\varepsilon_0 E_b} = \Psi_c(Q') \qquad (2.3)$$

This gives a nonlinear set of equations which give a nonlinear wave equation for Q' as

$$\frac{1}{L'}\,\frac{\partial^2}{\partial z^2}\left(\frac{Q'}{C'(Q')}\right) - \frac{\partial^2 Q'}{\partial t^2} = 0 \qquad (2.4)$$

which admits solutions of the form

$$Q' = Q'(\tau)$$
$$\tau = t \pm \frac{z}{v(Q')}$$

$$v(Q') = \left\{ \frac{1}{L'} \frac{d}{dQ'} \left[\frac{Q'}{C'(Q')} \right] \right\}^{\frac{1}{2}} \tag{2.5}$$

The current is in turn found from

$$\begin{aligned} \frac{dI(\tau)}{d\tau} &= \mp\, v(Q'(\tau)) \frac{dQ'(\tau)}{d\tau} \\ I(\tau) - I_i &= \mp \int_{Q'_i}^{Q'(\tau)} v(q')\, dq' \end{aligned} \tag{2.6}$$

with appropriate initial conditions.

Noting that speed $v(Q')$ decreases as $|Q'|$ increases, it is observed in [1] that as $|Q'|$ increases in the growth of the charge near a leader tip, the speed tends toward zero, thereby choking off the leader growth. This gives some kind of limitation on the growth of the leader tip into previously undisturbed air. There is also the question of the breakdown process at the very tip of the leader and how this may limit the propagation speed of the leader tip [3].

In [5] (2.6) is explicitly integrated to give a relation between I and Q', but this need not concern us here. More significantly, if we have a depletion (discharge) of the corona Q' back into the central arc as happens in a return stroke, then the speed increases during the discharge. This leads to the formation of an electromagnetic shock wave. Behind the shock front the propagation speed tends toward

$$c = [\mu_0 \varepsilon_0]^{-\frac{1}{2}} \equiv \text{speed of light} \tag{2.7}$$

as $\Psi_c \to \Psi_0$. In front of the shock the speed is much slower for $\Psi_c >> \Psi_0$. There we find the approximate solution

$$\beta = \frac{v}{c} \simeq \ell n^{-\frac{1}{2}} \left(\frac{\Psi_\infty}{\Psi_0} \right) = \ell n^{-\frac{1}{2}} \left(\frac{Q'_\infty}{Q'_0} \right) \tag{2.8}$$

Fortunately, for large argument the logarithm is very insensitive to the exact values of Ψ_∞ and Ψ_0. For $\Psi_\infty / \Psi_0 \simeq 10^4$ this gives $v \simeq c/3$ and large changes in Ψ_∞ / Ψ_0 change this result very little. Thus the model actually *predicts* the experimentally observed return-stroke speed.

It would be quite interesting if such a shock solution had some application in leader modelling. Characteristic times in a leader pulse are considerably shorter than in a return stroke [2, 4, 9] thereby reducing Ψ_∞. However, as we have seen, the shock speed is rather insensitive to Ψ_∞ / Ψ_0. Also one does not expect to have an almost total depletion of the charge behind the leader tip during a leader pulse. However, this does point in an interesting direction.

3. Forward and Backward Propagating Current in Leader Pulse

As indicated in Fig. 3.1A, consider some simplified initial conditions near a leader tip taken at $z_s = 0$ (s for source). Here the leader is propagating downward (into negative z_s), but this could apply to any direction (upward, sideward). The current is taken as from a negatively charged leader but it can be positive as well with simple sign changes. Initially the current is assumed as small (negligible) compared to that in the subsequent pulse. There is a corona containing the initial charge per unit length Q'_1 which is shown in a cylindrical form as constant for positive z_s and zero for negative z_s. Of course, near the tip the distribution of charge is not so discontinuous in radial distribution as in this model.

At some time, which we can take as $t = 0$, a current/charge pulse is initiated at $z_s = 0$ as indicated in Fig. 3.1B. The forward (downward) propagating current I_f is in a channel of length $|z_f|$ with

$$\begin{aligned} z_f &= -v_f t\ u(t) \\ v_f &\equiv \text{forward speed (positive)} \\ Q'_f &= -\frac{I_f}{v_f}\ u(v_f t + z_s)\ \text{(forward charge per unit length)} \end{aligned} \tag{3.1}$$

There is also a backward (upward) propagating current I_b in a channel of length z_b with

$$\begin{aligned} z_b &= v_b t\ u(t) \\ v_f &\equiv \text{backward speed (positive)} \\ Q'_b &= -\frac{I_b}{v_b}\ u(v_b t - z_s)\ \text{(backward charge per unit length)} \end{aligned} \tag{3.2}$$

Of course this Q'_b has to be added to Q'_1 (a decrease in magnitude due to opposite signs) to give the net charge per unit length behind the initial leader tip. The spatial form of the current is

$$\begin{aligned} I_f(z_s,t) &= I_f\ u(v_f t + z_s)\ \text{for}\ z_s < 0 \\ I_b(z_s,t) &= I_b\ u(v_b t - z_s)\ \text{for}\ z_s > 0 \end{aligned} \tag{3.3}$$

Continuity of current at $z = 0$ requires

$$I_f = I_b = I \tag{3.4}$$

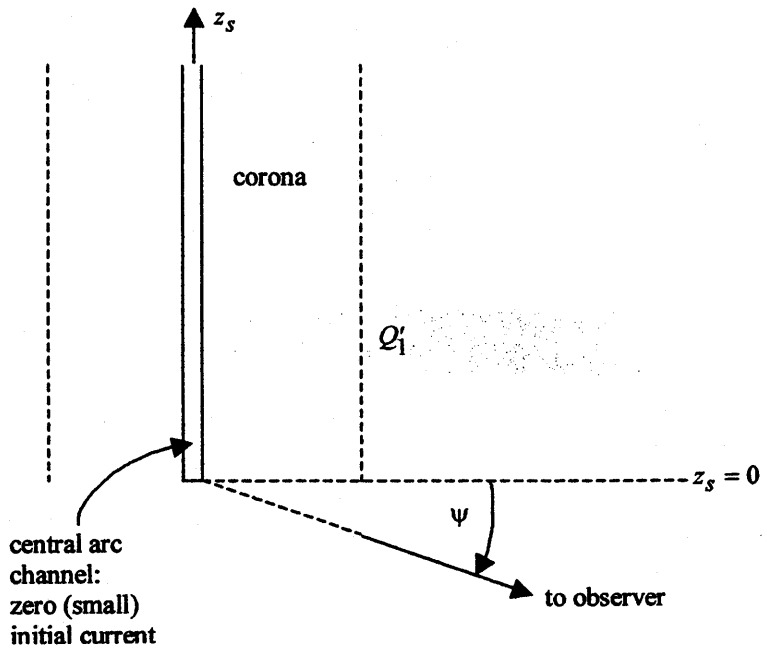

A. Initial conditions

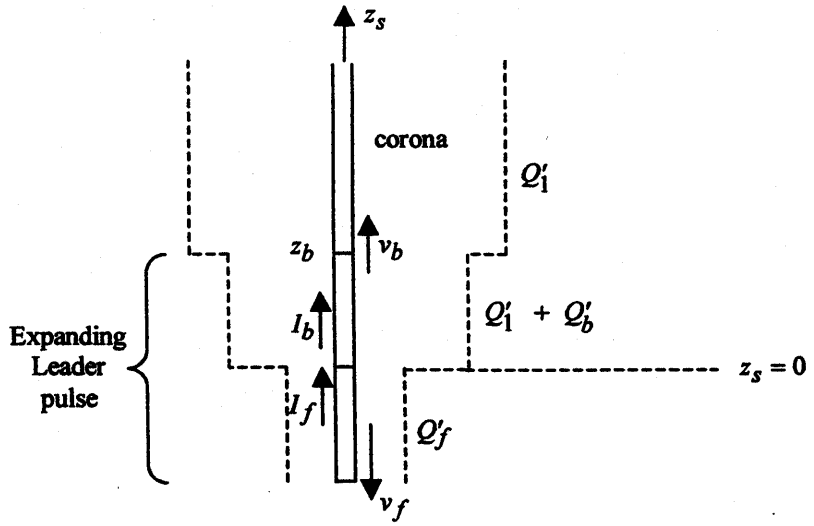

B. Leader-pulse conditions

Fig. 3.1. Model of Leader-Tip Extension

Note that the total charge in the leader must be zero (conservation of charge) so that

$$\begin{aligned} Q'_f|z_f| + Q_b z_b &= 0 \\ Q'_f\ v_f + Q_b\ v_b &= 0 \\ \frac{v_f}{v_b} &= -\frac{Q_b}{Q'_f} \end{aligned} \tag{3.5}$$

relating the speeds and charges per unit length.

Of course we have the bounds

$$\begin{aligned} &0 \le v_f \le c\ ,\quad 0 \le v_b \le c \\ &0 \le v_f + v_b \le 2c \end{aligned} \tag{3.6}$$

from causality. The forward speed v_f corresponds to a growing corona which decreases the speed. Furthermore, the breakdown process at the leader tip into the undisturbed air can further limit v_f. The backward speed v_b corresponds to a decreasing corona which leads in the direction of the shock solution discussed in the previous section. The backward propagation is also along an already-established conducting channel. Thus one may suspect that v_b is larger than v_f.

4. Radiated Field from Leader Pulse

The electric field (far field) radiated from a small source region is simply [2, 4, 9]

$$\vec{E}(t) = -\frac{\mu_0}{4\pi r} \overleftrightarrow{1}_t \cdot \vec{\Upsilon}(t - r/c)$$

$$\vec{\Upsilon}(t) = \frac{\partial}{\partial t} \int_{V'} \vec{J}\left(\vec{r}', t + \frac{1}{c}\left[r - \vec{1}_r \cdot \vec{r}' \right] \right) dV' \equiv \text{effective source vector}$$

$r = |\vec{r}| \equiv$ distance from observer to source

$\vec{r} \equiv$ coordinates of source center relative to the observer at coordinate origin (4.1)

$\vec{1}_r \equiv \frac{\vec{r}}{r} \equiv$ unit vector pointing from observer to source

$\overleftrightarrow{1}_t \equiv \overleftrightarrow{1} - \vec{1}_r \vec{1}_r$ (transverse unit dyadic)

$V' \equiv$ source volume

As indicated in Fig. 3.1, the observer is considered to be located at an angle ψ below the $z_s = 0$ plane. (The $z_s = 0$ plane need not be horizontal. Here "below" means in the negative z_s direction.)

From (3.3) we have the form of the current. Noting the effect of retarded time in (4.1) we have

$$\vec{\Upsilon}(t) = \vec{1}_{z_s} \Upsilon(t)$$

$$\Upsilon(t) = \frac{\partial}{\partial t}\left[\int_{-\infty}^{0} I\, u\left(v_f \left[t - \frac{1}{c} z_s \sin(\psi) \right] + z_s \right) d z_s + \int_{0}^{\infty} I\, u\left(v_b \left[t - \frac{1}{c} z_s \sin(\psi) \right] - z_s \right) d z_s \right]$$

$$= I \frac{\partial}{\partial t}\left[u(t) \left(\int_{-v_f t\left[1 - \frac{v_f}{c}\sin(\psi)\right]^{-1}}^{0} u(t)\, dz_s \right) + u(t) \left(\int_{0}^{v_b t\left[1 + \frac{v_b}{c}\sin(\psi)\right]^{-1}} dz_s \right) \right]$$

$$= I \left[v_f \left[1 - \frac{v_f}{c}\sin(\psi) \right]^{-1} + v_b \left[1 + \frac{v_b}{c}\sin(\psi) \right]^{-1} \right] u(t) \qquad (4.2)$$

The transverse dyadic alters the result as

$$\begin{aligned} \overleftrightarrow{1}_t \cdot \vec{\Upsilon}(t) &= \overleftrightarrow{1}_t \cdot \vec{1}_{z_s} \Upsilon(t) \\ |\vec{1}_t \cdot \vec{1}_{z_s}| &= \cos(\psi) \end{aligned} \tag{4.3}$$

with direction (polarization) perpendicular to $\vec{1}_r$ and in the plane containing the z_s axis. So we have

$$\cos(\psi)\Upsilon(t) = I\cos(\psi)\left[v_f\left[1-\frac{v_f}{c}\sin(\psi)\right]^{-1} + v_b\left[1+\frac{v_b}{c}\sin(\psi)\right]^{-1}\right]u(t) \tag{4.4}$$

For convenience we have the simpler case

$$\begin{aligned} \psi &= 0 \\ \Upsilon_0(t) &= \left[\cos(\psi)\,\Upsilon(t)\right]_{\psi=0} \\ &= I\left[v_f + v_b\right]u(t) \end{aligned} \tag{4.5}$$

Here $\cos(\psi)$ is maximized but other factors can be maximized for other values of ψ. For ψ near $\pi/2$, if v_f/c is near 1 the forward leader pulse has enhanced radiation. For ψ near $-\pi/2$ the backward leader pulse also gives enhanced radiation. However, for simple order-of-magnitude estimates

$$\Upsilon_0 = I\left[v_f + v_b\right] \tag{4.6}$$

should be useful.

Considering the experimental data [2, 4, 9] one finds that Υ_0 lies in the range of 10^{11} to 10^{12} Am/s, the larger number being occasionally slightly exceeded. Of course there are errors in the data, primarily in the estimate of r the distance from the observer (Kiva 1) to the source region. This estimate is obtained from whole-sky videotape photographs, thunder delays, time of arrival of electromagnetic signals at three different antenna locations, and the polarization of successive pulses of $\overleftrightarrow{1}_t \cdot \vec{\Upsilon}$ as measured by two B-dot and one D-dot sensors. We expect better than a factor of 2 for the estimate of r which should be fine for order-of-magnitude estimates. There is also the question of the orientation of $\vec{\Upsilon}$ as it is only the transverse part that one measures and there is some additional effect of $\sin(\psi)$ in (4.4).

Take the number of 10^{12} Am/s to consider some estimates of currents and speeds as

$$I\left[v_f + v_b\right] = \Upsilon_0 \equiv 10^{12}\ \text{Am/s} \tag{4.7}$$

From the bound in (3.6) we have

$$\begin{aligned} &v_f + v_b \le 2c \\ &I \ge \frac{\Upsilon_0}{2c} \simeq 3.3\ \text{kA} \end{aligned} \tag{4.8}$$

which does not seem unreasonable. If we can neglect v_f compared to v_b we would have

$$I \ge \frac{\Upsilon_0}{c} \simeq 6.7\ \text{kA} \tag{4.9}$$

If we were to further estimate v_b by the return-stroke speed we would have

$$\begin{aligned} &v_b \simeq \frac{1}{3}c \quad , \quad v_f \simeq 0 \\ &I \ge 3\frac{\gamma_0}{c} \simeq 20\ \text{kA} \end{aligned} \tag{4.10}$$

which is maybe getting a little large. However, one should remember that Υ_0 can often be one decade lower. So, while these results don't establish the current and speeds they do give a product in which I, v_f, and v_b can be traded off to see what is reasonable and even give some bounds.

5. Enhancement of Leader-Tip Speed During Leader Pulses as Seen in Data

In our discussion of the leader pulses we have assumed that the leader progresses forward essentially only during these pulses. As in Fig. 3.1A, the charge (corona, Q'_1) has built up near the tip until the electric field there is sufficient to allow the breakdown of the air and the tip to propagate forward as in Fig. 3.2B. Then the pulse and forward movement of the tip is stopped for various reasons such as the choking phenomenon discussed in Section 2 in which v_f decreases as $|Q'_1|$ increases. Furthermore, we have neglected the resistance per unit length in the arc which will attenuate (and disperse) the current wave. There is also some limiting of v_f by the breakdown process at the tip, and as the electric field drops the breakdown is stopped until enough charge can build up to restart the pulsing process.

Note that there is some continuing current coming from farther back on the leader, limited also by the leader resistance per unit length. It is this current which rebuilds the charge and electric field near the leader tip. This smaller current (compared to the leader-pulse current) also radiates fields to the observer, but the slower time scale for this contribution allows one to distinguish this slower component from the contributions from the relatively fast leader pulses.

If the average forward speed of the leader tip (averaged over a time window containing many leader pulses) is v_0, and the average time between such pulses is T_0, then we have

$$\eta_\ell \equiv \frac{\text{average } v_f \text{ in leader pulses}}{\text{average } v_0 \text{ of leader trip}} \equiv \frac{v_f}{v_0}$$

$$= \frac{T_0}{T_f} \equiv \text{speed enhancement factor in leader} \tag{5.1}$$

$$T_f \equiv \text{average width (in time) of leader pulse}$$

Said another way

$$v_f \; T_f = v_0 \; T_0 \equiv \text{average tip distance advanced during leader pulse} \tag{5.2}$$

So now one can look at experimental data. Figures 5.1 and 5.2 are taken from [2] and also appear in [9]. Here we have a good example of fast pulses occurring against a slower background. In going from the digital record of the time derivative of the fields in Fig. 5.1 to the fields in Fig. 5.2 there are some integration errors which may contribute to the slow variation, but have less effect on the superimposed fast pulses. This event was triggered by a rocket at about 600 m above Kiva 1 and zenith angle $\theta \simeq 30°$ with azimuth $\phi \simeq 155°$ (a little east of sourth). The

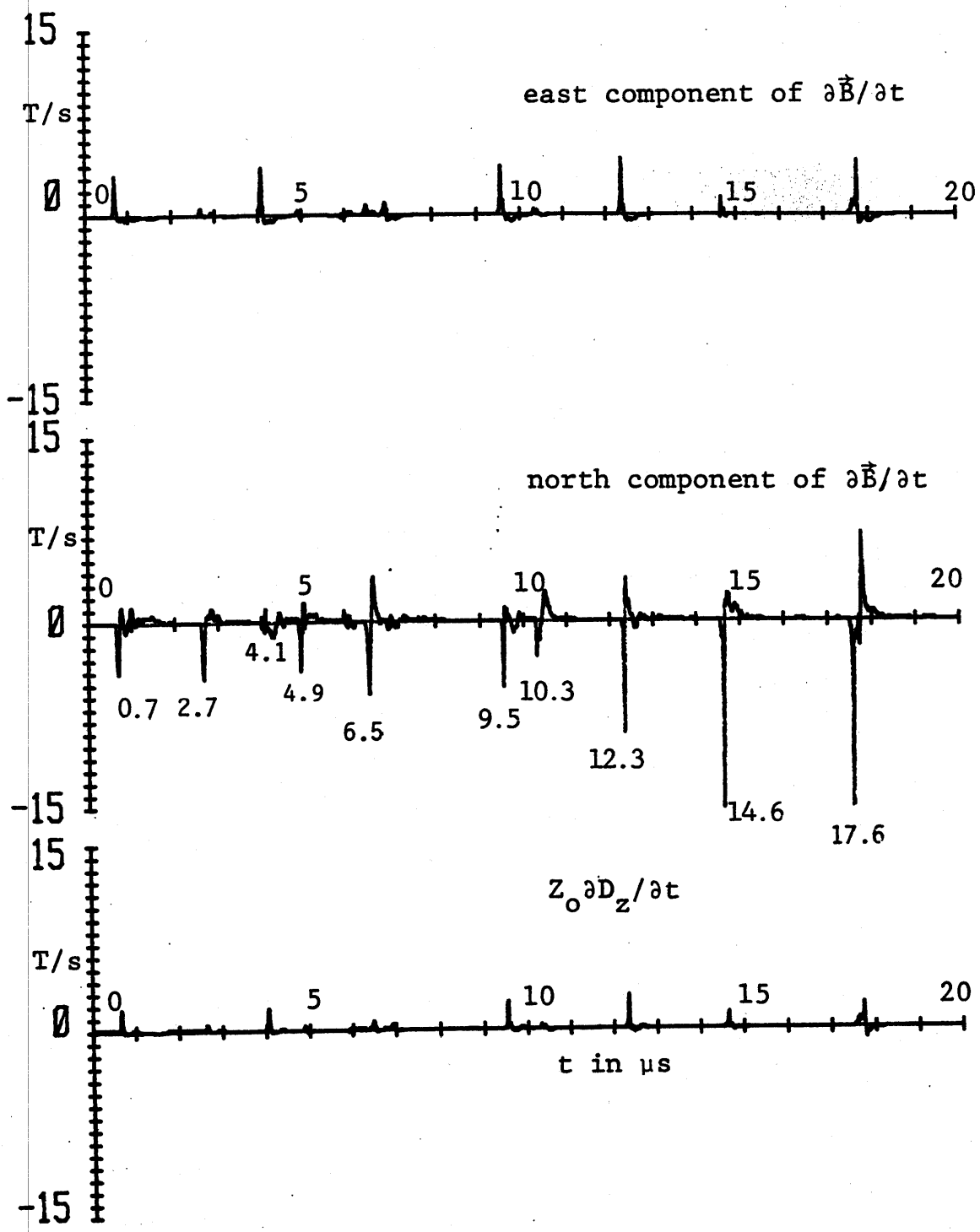

Fig. 5.1. Derivative Fields From Rocket-Triggered Lightning.

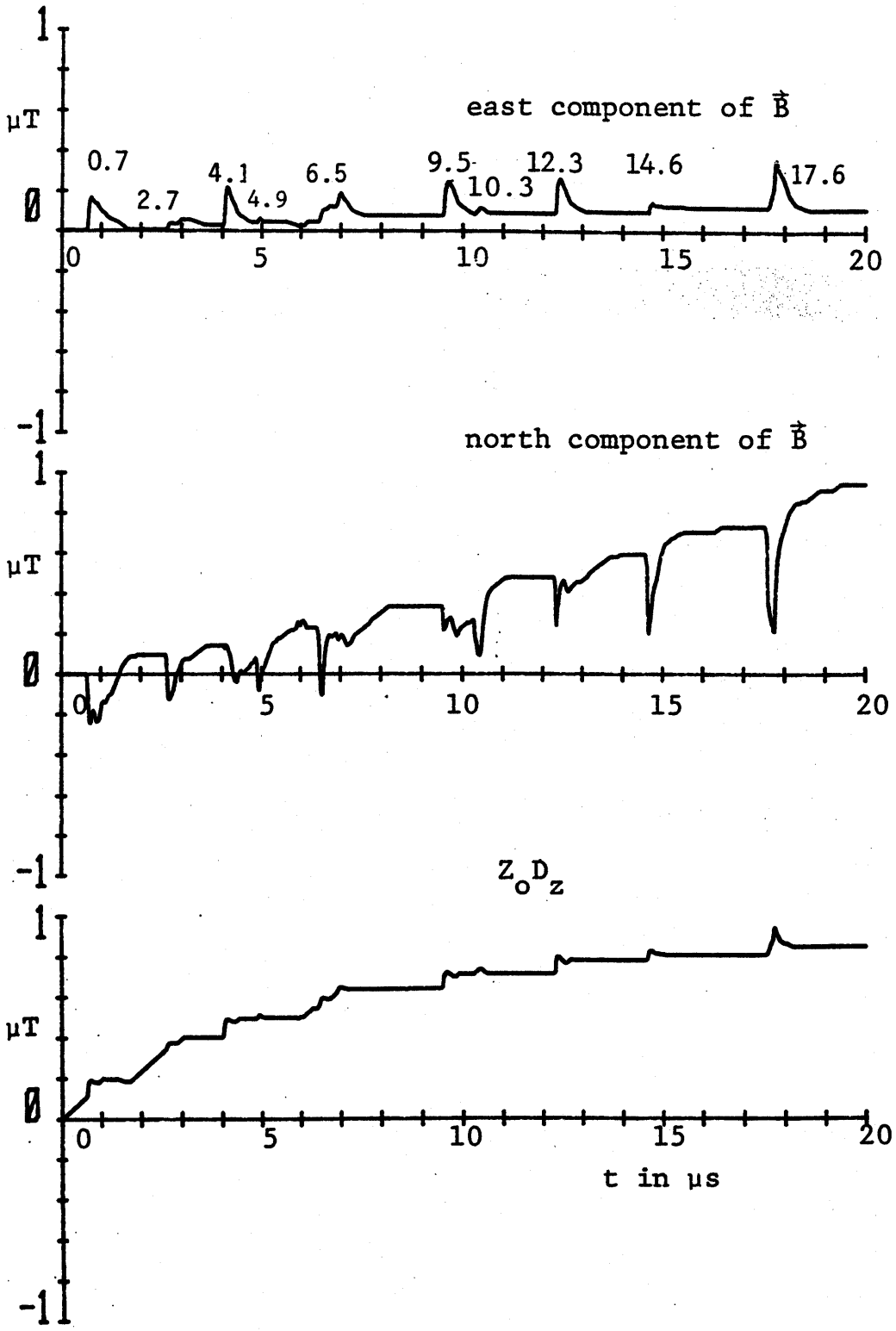

Fig. 5.2. Fields From Rocket-Triggered Lightning.

estimated source location is $(r, \theta, \phi) \simeq$ (915 m, 22.5°, 173°) which is discussed in detail in [2]. This appears to be a positive streamer propagating "upward" from the rocket.

Figures 5.3 and 5.4 show the peaks of $\partial \overleftrightarrow{1}_t \cdot \vec{\Upsilon}/\partial t$ and $\overleftrightarrow{1}_t \cdot \vec{\Upsilon}$ respectively, remembering that the sensors only record the transverse part. Note the strong horizontal component (rightward) as seen from the observer (usual h, v coordinates). This is also seen from the strongest field component being the north magnetic field in Figs. 5.1 and 5.2. Note that all three field components are appropriately normalized to have the same units so their amplitudes can be readily compared. Besides the transverse projection of the leader pulses indicating the shape of the leader (upper parts of Figs. 5.3 and 5.4), we can note the progressively increasing strengths of the leader pulses as the leader propagates "upward" to meet the leader coming "downward" from the cloud. So there might be included some pulses from the downward negative leader if the two leaders are sufficiently close in approach. For a single leader this would increase the average time T_0 between pulses.

Let us estimate T_f from (5.1) in this data. There are various ways one might do this from the detailed digital waveform data in [2]. For our purposes of order-of-magnitude estimates (not trying to go beyond about one significant figure) we can estimate this for each pulse as

$$T_f \simeq \frac{\text{peak of} \left| \overleftrightarrow{1}_t \cdot \vec{\Upsilon}(t) \right|}{\text{peak of} \left| \frac{\partial}{\partial t} \overleftrightarrow{1}_t \cdot \vec{\Upsilon}(t) \right|} \tag{5.2}$$

Taking the eight largest pulses and using the magnitudes of the vectors in the lower portions of Figs. 5.3 and 5.4, we find T_f varying from about 20 ns to 50 ns with a mean of roughly 40 ns. The three largest pulse in the right end of the record give about 20 ns. The eight pulses in 20 μs give a T_0 of about 2.5 μs. This gives a speed enhancement factor

$$\eta_\ell \simeq \begin{cases} 80 \text{ averaged over 8 pulses} \\ 125 \text{ averaged over last 3 "large" pulses} \end{cases} \tag{5.3}$$

Anyway, in an order-of-magnitude sense η_ℓ is about 100 from this data. One can look at the rest of the data [2, 4] to observe roughly similar behavior, even with the variability.

As discussed in Section 1, the average speeds of leaders have been optically measured to lie in the general range of 10^5 to 10^6 m/s. If we combine this with the speed enhancement factor of about 100 for the ratio of step v_f to average speed, we obtain values of v_f in the range of 10^7 to 10^8 m/s. This is less than the bound of c, and

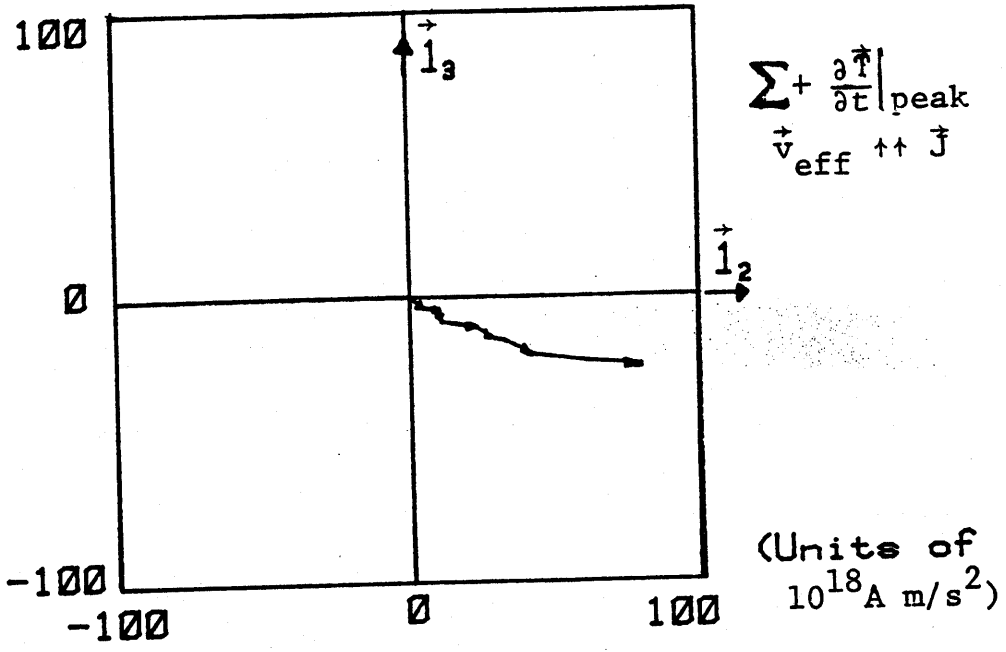

Effective reconstruction of positive streamer

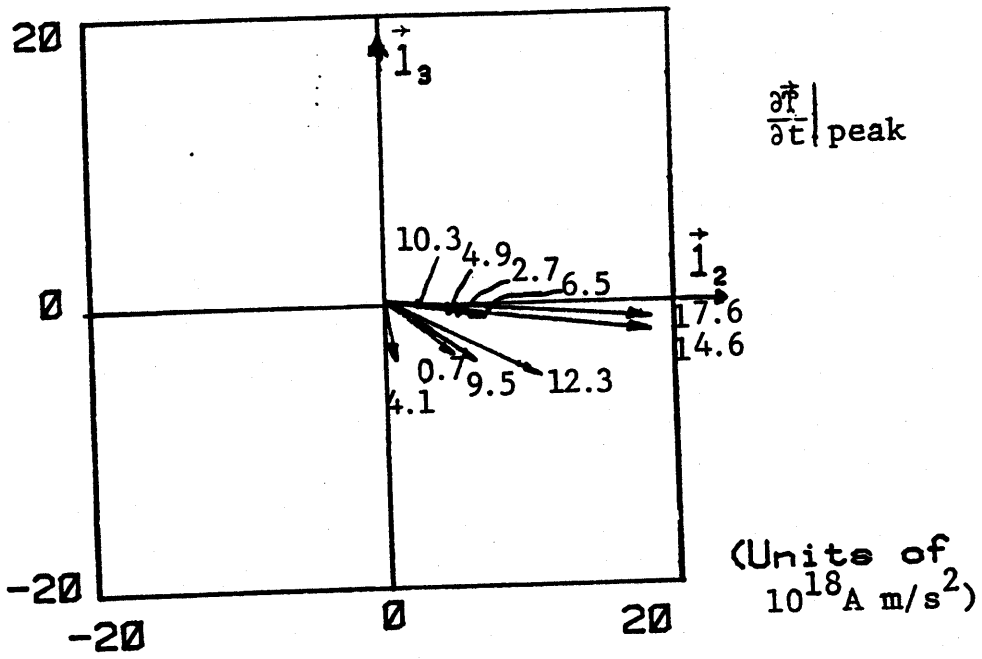

Peaks of $\partial \vec{T}/\partial t$

$\phi = 172.7^0$, $\theta = 22.5^0$, $r = 915$ m

Fig. 5.3. $\partial \vec{T}/\partial t$ for Rocket-Triggered Lightning.

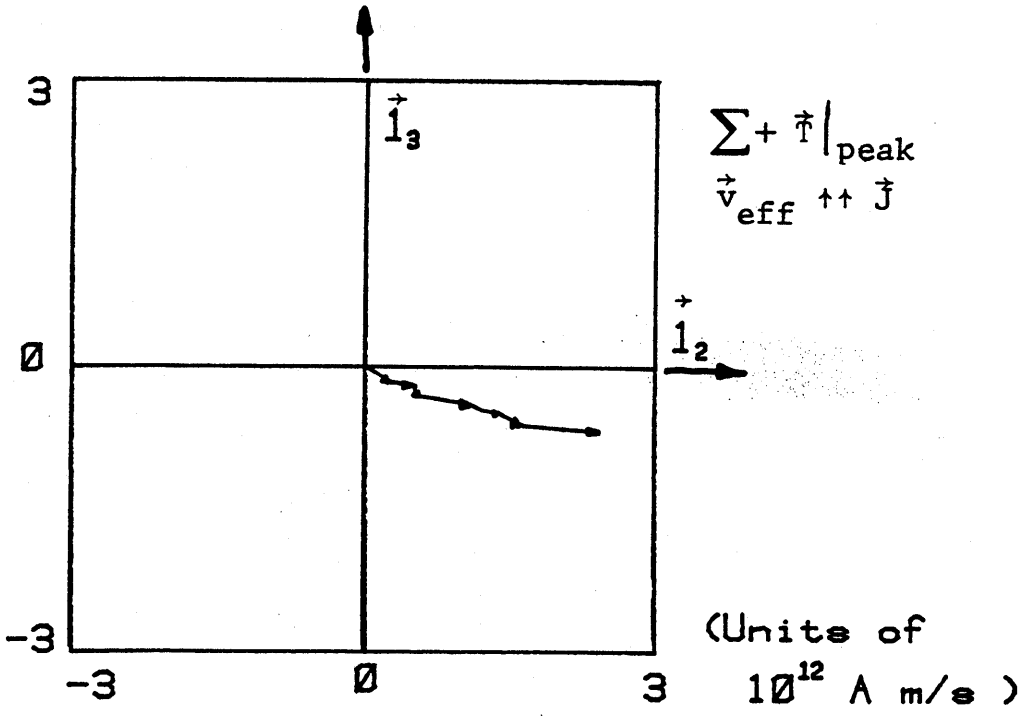

Effective reconstruction of positive streamer

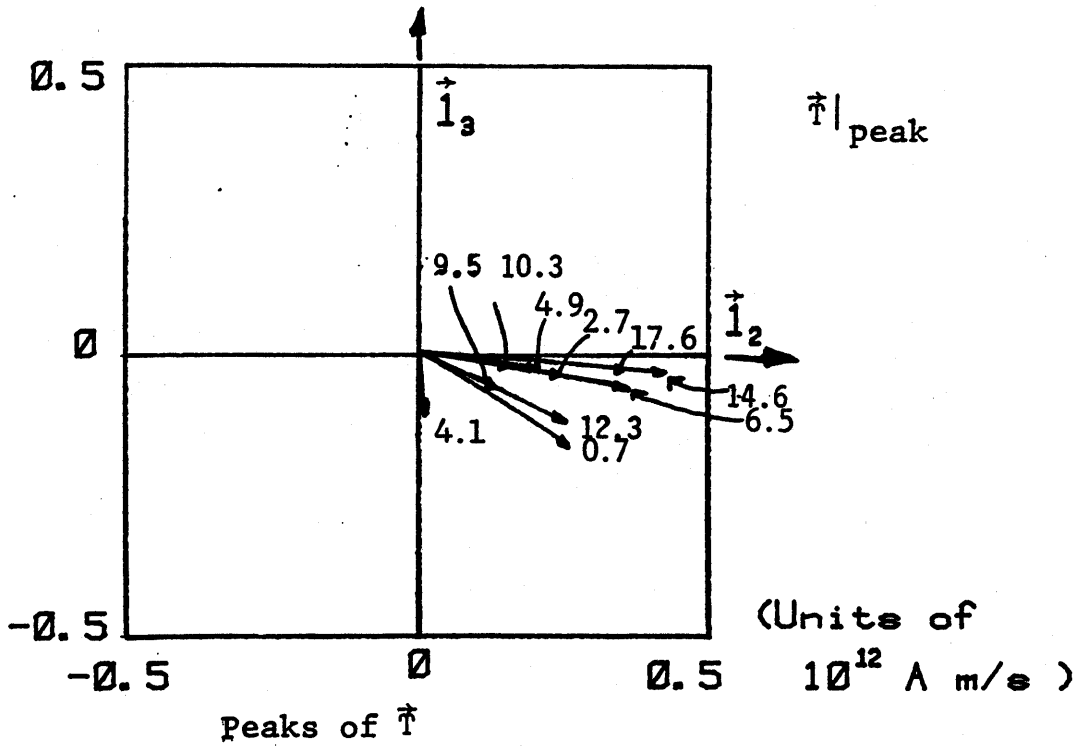

Peaks of $\vec{T}$

$\phi = 165.8^{o}$, $\theta = 16.1^{o}$, $r = 1262$ m

Fig. 5.4. $\vec{Y}$ for Rocket-Triggered Lightning.

consistent with the model in Section 3 and reasonable currents as discussed in Section 4. It is also consistent with the estimates of step speeds using limited-time-resolution photography in the cited references.

Note also in this data that the pulses are significantly increasing in intensity as time progresses. This may be associated with close approach of upward and downward leaders with accompanying higher electric fields. This may also be associated to the few microsecond times between the pulses. A longer recording time would have been helpful in this case.

6. Concluding Remarks

Above all, one needs to recognize that the numbers developed herein are order-of-magnitude estimates based on an approximate model of the currents and speeds in the leader pulse based on the corona nonlinear-transmission-line model. Fundamental to these estimates is the ratio of leader-tip speed during the fast step to the speed averaged over many steps. This ratio estimate would be decreased if there were significant but slow leader-tip advance between the leader pulses. Note this and other assumptions used in constructing the model. This is tempered by the constraint of c on the various speeds and reasonable values of I during the pulses.

The fast electromagnetic data is used to estimate the tip-speed ratio. It would be useful to have more and better such data. The time resolution of the electromagnetic waveforms can be improved using transient-waveform digitizers currently available. Perhaps this can be combined with appropriate optical data.

We can note that the speed of current propagation and the speed associated with the optical emission along the channel are not necessarily the same, depending on various conditions. The current wave tends to precede the optical response to the current, and how much delay there is between the two depends on the time to heat the channel (I^2R' heating) to temperatures hot enough for significant optical emission. This heating time then depends on the characteristics of the current I (amplitude, rise time, etc.) as well as the resistance per unit length R' of the channel as a function of time. (There are also other energy losses due to hydrodynamic and chemical processes.) This deserves further investigation (into the sub-100 ns regime) to better quantify the relation between current and optical emission.

Acknowledgement: I would like to thank Prof. V. A. Rakov of the University of Florida for providing me some of the references and for discussions concerning them.

References

1. C. E. Baum, Properties of Lightning-Leader Pulses, Lightning Phenomenology Note 2, December 1981; pp. 3-16, in R. L. Gardner (ed.), *Lightning Electromagnetics*, Hemisphere (Taylor & Francis), 1990.

2. C. E. Baum, E. L. Breen, J. P. O'Neill, C. B. Moore, and D. L. Hall, Measurements of Electromagnetic Properties of Lightning with 10 Nanosecond Resolution, Lightning Phenomenology Note 3, February 1982.

3. C. E. Baum and R. L. Gardner, An Introduction to Leader-Tip Modeling, Lightning Phenomenology Note 5, July 1982; pp. 41-45, in R. L. Gardner (ed.), *Lightning Electromagnetics*, Hemisphere (Taylor & Francis), 1990.

4. C. E. Baum, J. P. O'Neill, E. L. Breen, D. L. Hall, and C. B. Moore, Location of Lightning Electromagnetic Sources by Time of Arrival Compared to Inference from Electromagnetic Fields, Thunder Acoustics, and Videotape Photographs, Lightning Phenomenology Note 11, October 1983.

5. C. E. Baum and L. baker, Return-Stroke Transmission-Line Model, Lightning Phenomenology Note 13, October 1984; Analytic Return-Stroke Transmission-Line Model, pp. 17-40, in R. L. Gardner (ed.), *Lightning Electromagnetics*, Hemisphere (Taylor & Francis), 1990.

6. B. F. J. Schonland, The Lightning Discharge, pp. 576-628, *Handbuch der Physik*, Vol. 22, Springer-Verlag, 1956.

7. K. Berger, Novel Observations on Lightning Discharges: Results of Research on Mount San Salvatore, J. Franklin Institute, Vol. 283, No. 6, June 1967, pp. 478-525.

8. V. P. Idone, The Luminous Development of Florida Triggered Lightning, Res. Lett. Atmos. Electr., Vol. 12, 1992, pp. 23-28.

9. C. E. Baum, J. P. O'Neill, E. L. Breen, D. L. Hall, and C. B. Moore, Electromagnetic Measurement and Location of Lightning, pp. 319-346, in R. L. Gardner (ed.), *Lightning Electromagnetics*, Hemisphere (Taylor & Francis), 1990.

10. V. A. Rakov, *Lightning*, Univ. of Florida (course notes), 1998.